# Effect of porosity enhancing agents on the electrochemical performance of high-energy ultracapacitor electrodes derived from peanut shell waste

**N. F. Sylla [a], N. M. Ndiaye [a], B. D. Ngom [b], D. Momodu**

**M. J. Madito, B. K. Mutuma [a] and N. Manyala [a]***

[a] Department of Physics, Institute of Applied Materials, SARChI Chair in Carbon Technology and Materials, University of Pretoria, Pretoria 0028, South Africa

[b] Laboratoire d'Energie, de Photonique et de Nano-Fabrication, Faculté des Sciences et Techniques Université Cheikh Anta Diop de Dakar (UCAD) B.P. 25114 Dakar-Fann Dakar, Sénégal

*Corresponding author email: ncholu.manyala@up.ac.za, Tel: + (27)12 420 3549

Fax: + (27)12 420 2516

## Supporting information

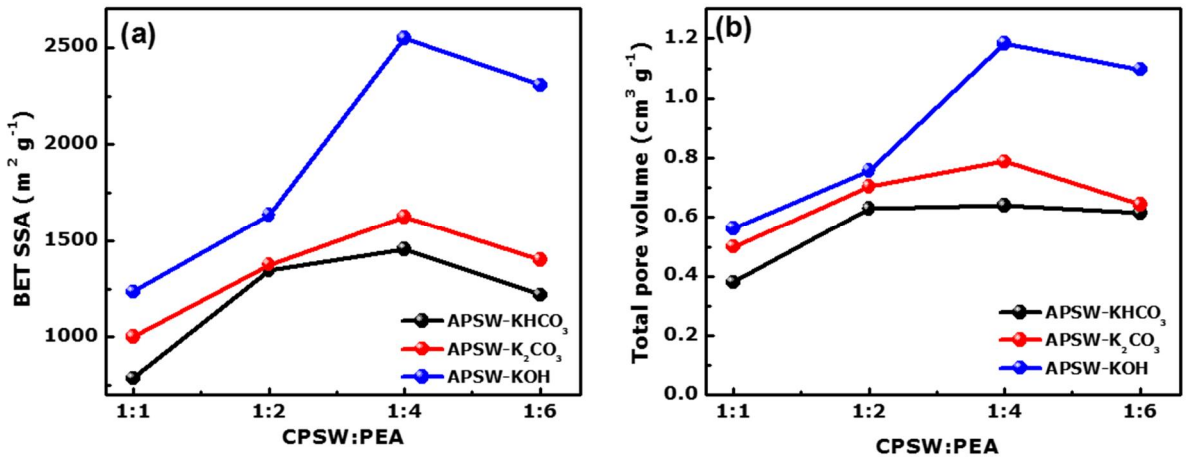


**Figure S1**: (a) The plot of specific surface area and (b) Total pore volume as a function of the APSW at different activated agent for different ratios.

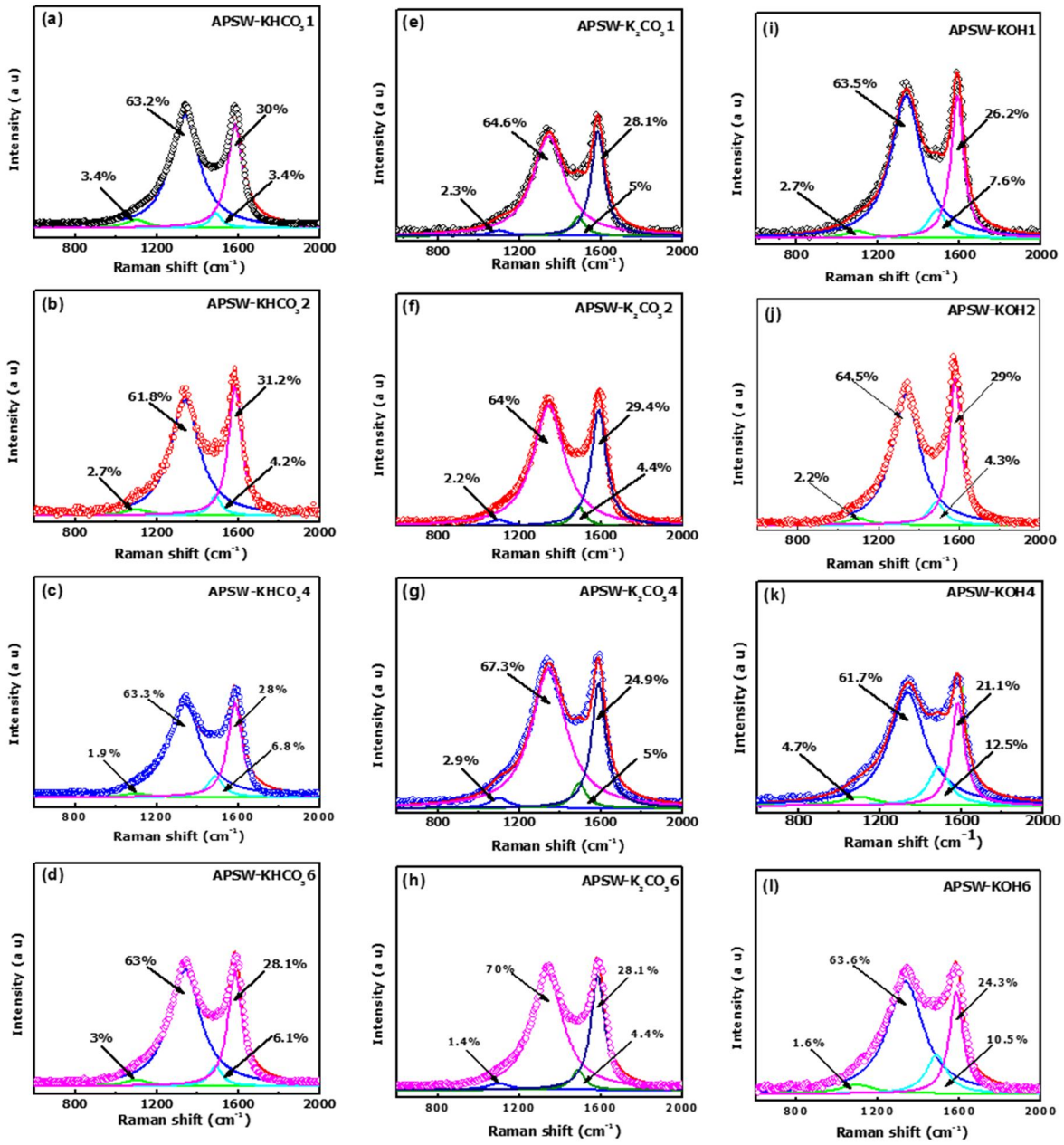


**Figure S2**. Deconvolution of the Raman spectra showing the integral areas of the D1, D, D2 and G peaks for all the APSW-Yx samples.

**Table S1**: Specific surface area (SSA) data of different APSW-Yx samples

| CPSW:PEA | SSA ($m^2$ $g^{-1}$) | | |
|---|---|---|---|
| | $KHCO_3$ | $K_2CO_3$ | KOH |
| **1:1** | 787 | 1002 | 1235 |
| **1:2** | 1348 | 1376 | 1637 |
| **1:4** | 1457 | 1625 | 2547 |
| **1:6** | 1219 | 1401 | 2306 |

**Table S2**: D/G ratio, effective crystallite size $L_a$ and D peak FWHM data of different APSW-Yx samples

| CPSW:PEA | D/G | | | $L_a$ (nm) = 4,96/(D/G)* | | | D peak FWHM ($cm^{-1}$) | | |
|---|---|---|---|---|---|---|---|---|---|
| | $KHCO_3$ | $K_2CO_3$ | KOH | $KHCO_3$ | $K_2CO_3$ | KOH | $KHCO_3$ | $K_2CO_3$ | KOH |
| **1:1** | 2.1 | 2.3 | 2.4 | 2.4 | 2.2 | 2.1 | 170.3 | 183.4 | 192.7 |
| **1:2** | 2.0 | 2.2 | 2.2 | 2.5 | 2.3 | 2.3 | 160.1 | 169.3 | 187.1 |
| **1:4** | 2.3 | 2.7 | 2.9 | 2.2 | 1.8 | 1.7 | 194.6 | 206.4 | 225.7 |
| **1:6** | 2.3 | 2.7 | 2.6 | 2.2 | 1.8 | 1.9 | 187.2 | 201.9 | 215.7 |

* Equation adopted from [1]

**Table S3**: Atomic concentration data of the APSW-$KHCO_3$, APSW-$K_2CO_3$ and APSW-KOH at a mass ratio of 1 to 4 samples

| | Atomic Conc (%) | | |
|---|---|---|---|
| | C1S | O1S | N1S |
| **APSW-$KHCO_3$4** | 85.2 | 14.2 | 0.6 |
| **APSW-$K_2CO_3$4** | 86.9 | 11.9 | 1.2 |
| **APSW-KOH4** | 87.9 | 11.5 | 0.6 |

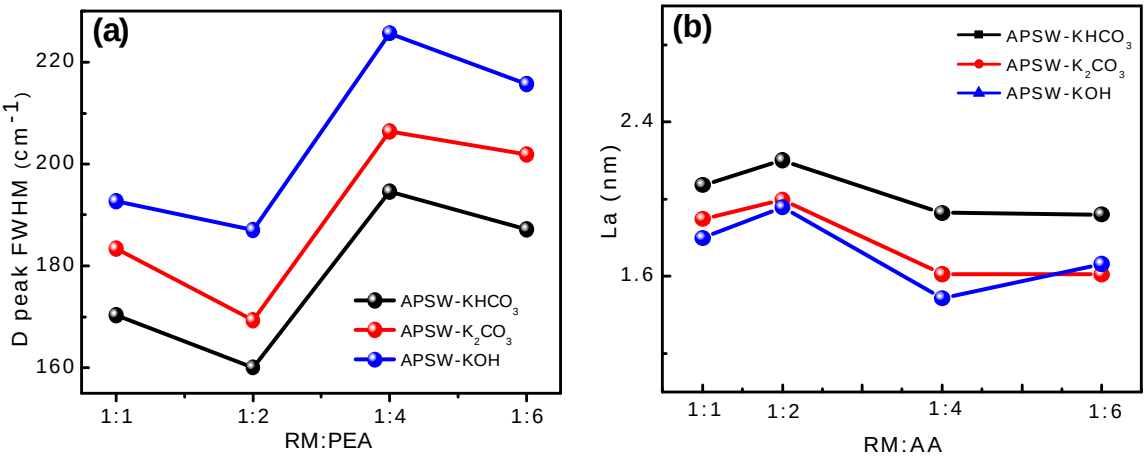


**Figure S3**. (a) D peak FWHM and (b) effective crystallite size $L_a$ as function of APSW-$KHCO_3$, APSW-$K_2CO_3$, APSW-KOH at different mass ratios.

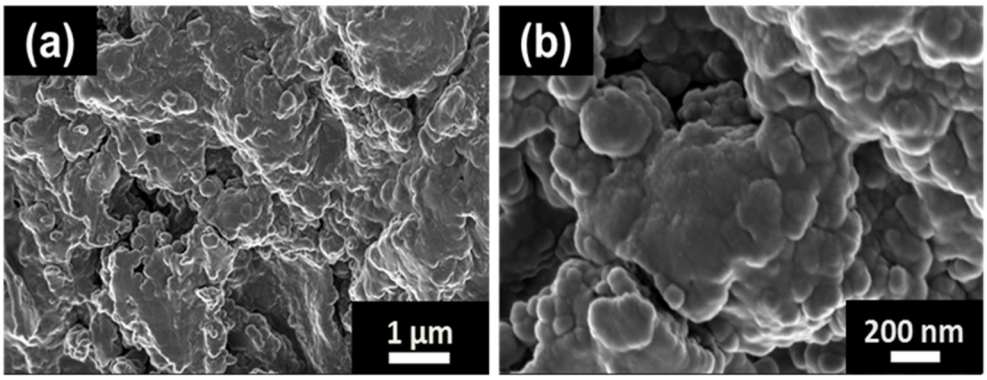


**Figure S4.** SEM images of the raw PSW at: (a) low and (b) high magnification

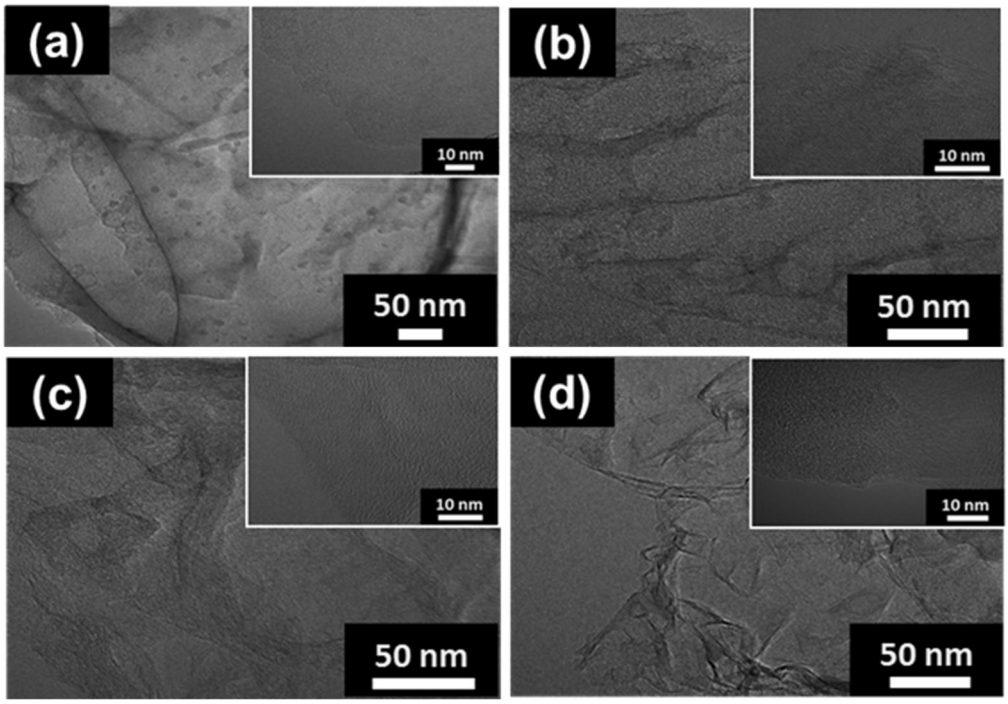


**Figure S5.** HRTEM images at low and high magnification (inset) of (a) CPSW; (b) APSW-$KHCO_3$4; (c) APSW-$K_2CO_3$4 and (d) APSW-KOH4

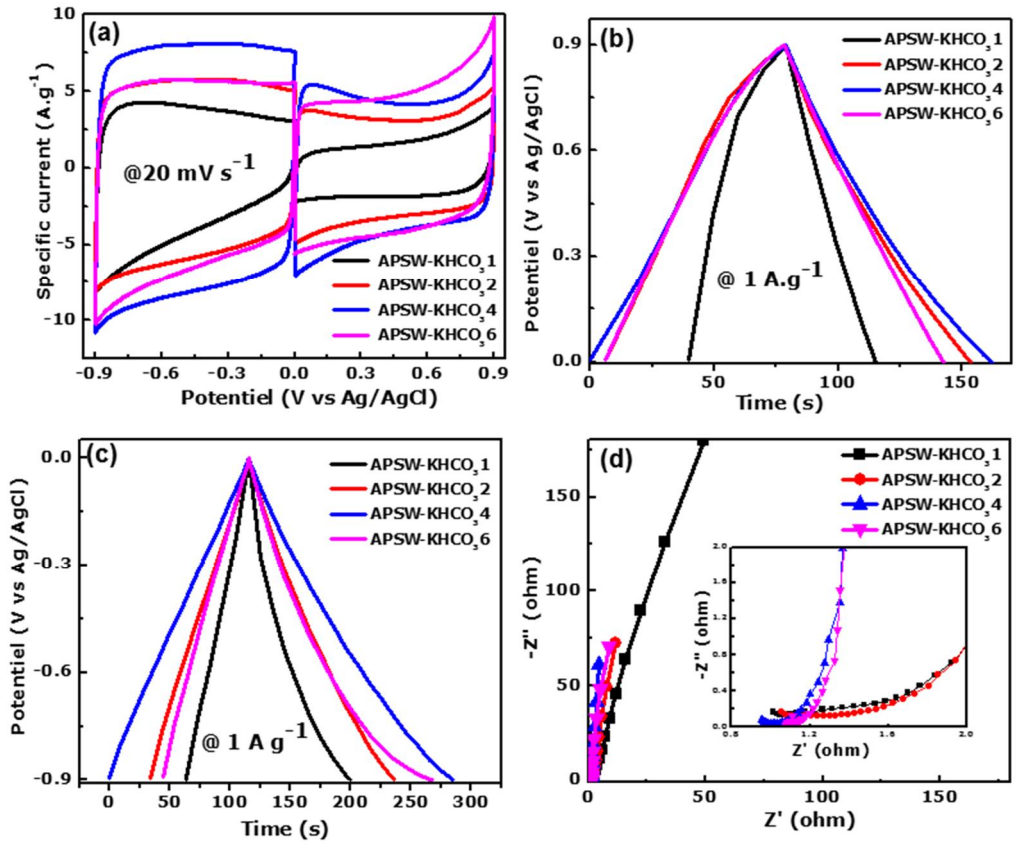


**Figure S6.** Electrochemical measurement of the APSW-$KHCO_3$ electrodes at different concentrations: (a) CV curves at a scan rates 20 mV $s^{-1}$, (b) and (c) GCD plots at a specific current of 1 A $g^{-1}$ in the positive and negative potential windows, respectively and (d) Nyquist plots.

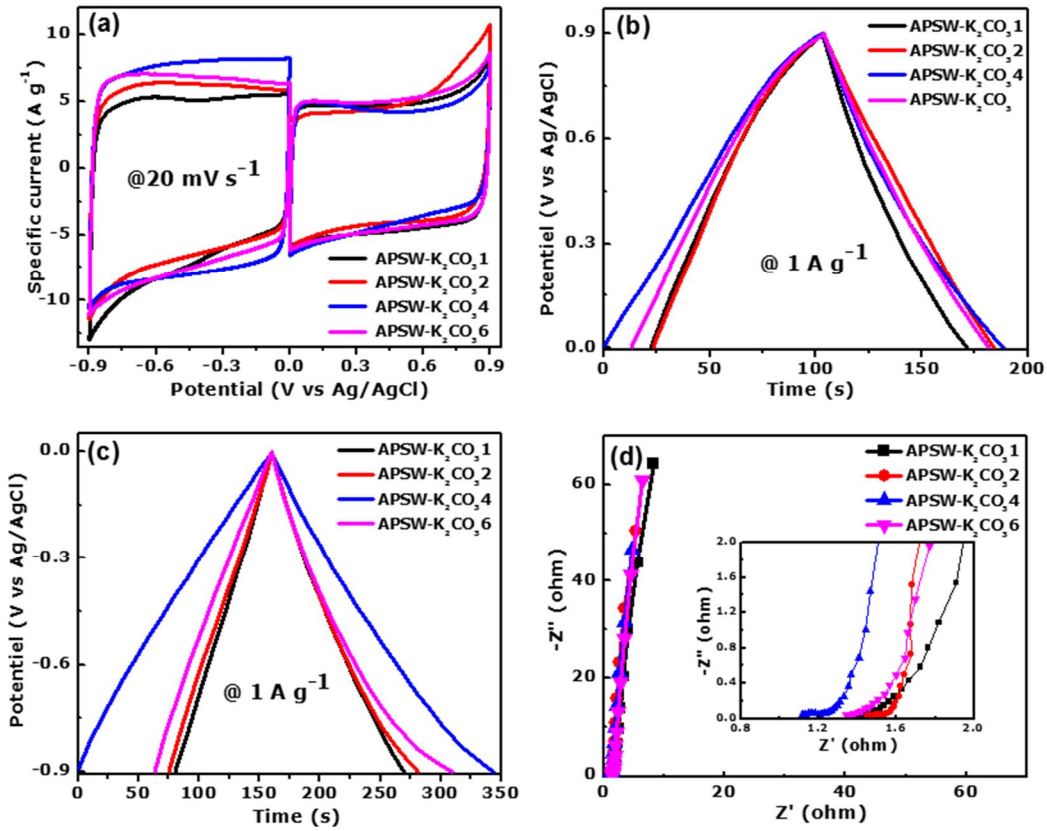


**Figure S7.** Electrochemical measurement of the APSW-$K_2CO_3$ electrodes at different concentrations: (a) CV curves at a scan rates 20 mV $s^{-1}$, (b) and (c) GCD plots at a specific current of 1 A $g^{-1}$ in the positive and negative potential windows, respectively (d) Nyquist plots.

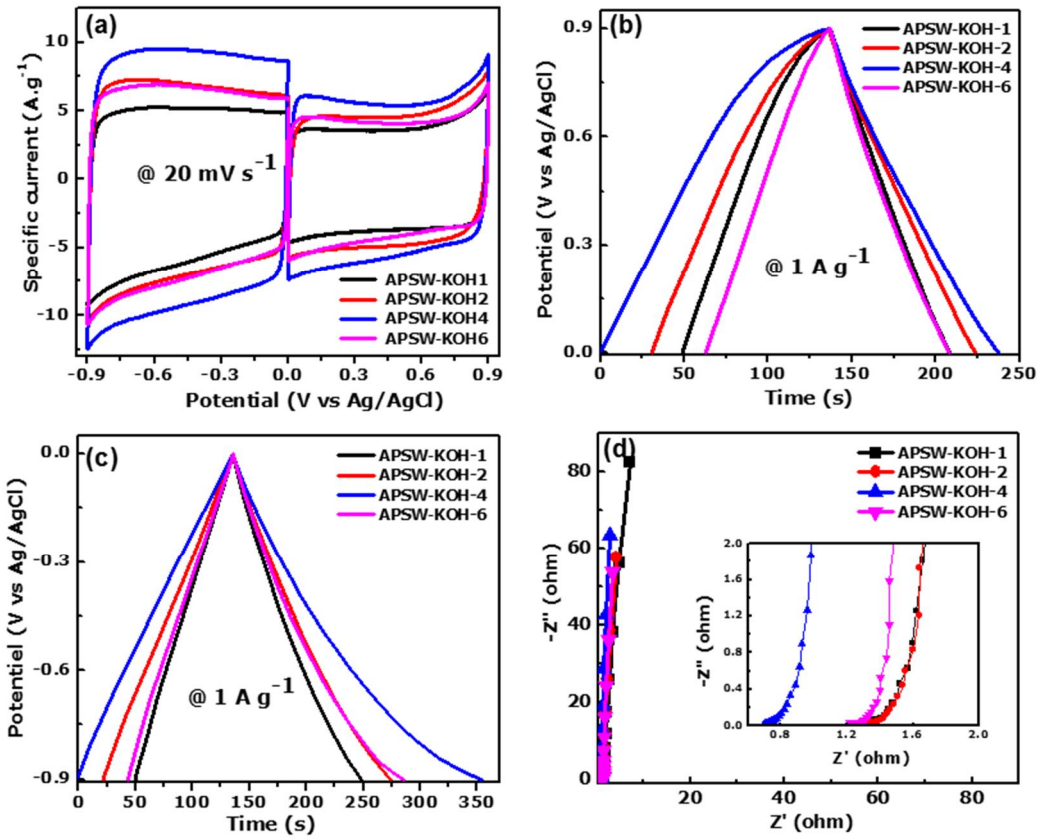


**Figure S8.** Electrochemical measurement of the APSW-KOH electrodes at different concentrations: (a) CV curves at a scan rates 20 mV $s^{-1}$, (b) and (c) GCD plots at a specific current of 1 A $g^{-1}$ in the positive and negative potential windows, respectively (d) Nyquist plots.

**Table S4.** EIS fitting parameters obtained from the complex non-linear least square (CNLS) method of the equivalent circuit shown in the inset to Fig. 6d

| **Electrode** | $R_s$ **(Ω)** | $R_{CT}$ **(Ω)** | *Q2* **(F)** | $R_L$ **(Ω)** |
|---|---|---|---|---|
| **APSW-KOH4 //APSW-KOH4** | 1.01 | 0.79 | 0.146 | $7.99 \times 10^2$ |
| $X/\sqrt{N}$ = 0.366, *Q2 ≡ leakage capacitance*, | | | | |

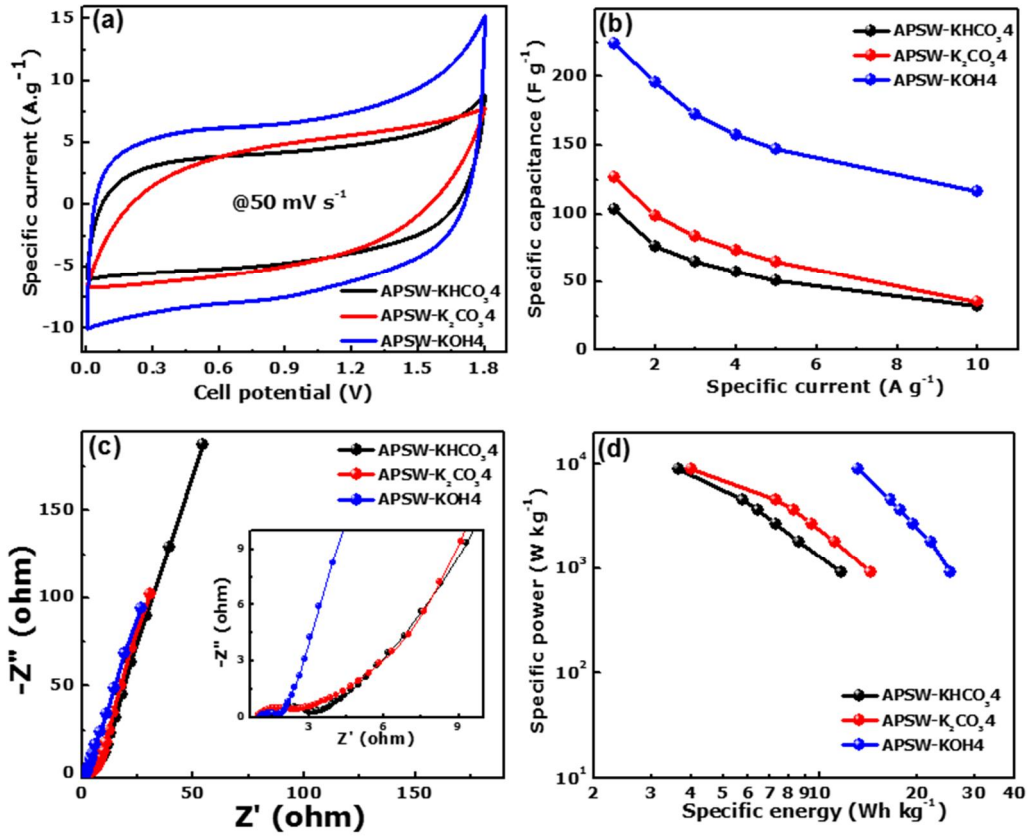


**Figure S9.** Comparison of the symmetric electrodes APSW-$KHCO_3$//APSW$KHCO_3$, APSW$K_2CO_3$//APSW$K_2CO_3$, APSW-KOH//APSW-KOH at a mass ratio 1:4: (a) CV curves, (b) specific capacitance as function of the specific current, (c) Nyquist plots and (d) Comparison of the Ragone plot for the three symmetric devices

## References

1. Endo, M. & Pimenta, M. A. Origin of dispersive effects of the raman d band in carbon materials. *Phys. Rev. B - Condens. Matter Mater. Phys.* **59,** R6585–R6588 (1999).